



Cite this: *React. Chem. Eng.*, 2022, 7, 711

Received 7th December 2021,
Accepted 15th December 2021

DOI: 10.1039/d1re00551k

rsc.li/reaction-engineering

Mechanistic investigations on a homogeneous ruthenium Guerbet catalyst in a flow reactor†

Nicholas M. Wang, Sam Dillon and Damien Guironnet *

A mechanistic investigation on the ethanol self-condensation reaction (Guerbet reaction) catalyzed by a bis(pyridylimino)isoindolate Ru(II) catalyst was performed using a specifically designed continuously-stirred tank reactor (CSTR). Leveraging vapor-liquid equilibrium, the homogeneous catalyst was maintained in the reactor at a constant concentration by dissolving it in a non-volatile solvent while volatile substrates were fed continuously. The activity of the catalyst was monitored by analyzing the vapor exiting the reactor (reagents and products) using an in-line gas chromatograph. The formation of C₆ products demonstrates the catalyst's reactivity towards butanol, and the detection of solely saturated products implies that hydrogenation is fast under the reaction conditions. These observations led us to perform a detailed study of the hydrogenation step that provided evidence for a hydrogen-transfer pathway. The corresponding reaction mechanism for the Guerbet reaction was established.

Introduction

The catalytic self-condensation of ethanol, referred to as the Guerbet reaction, presents an attractive route to convert the widely available bio-ethanol into a more advanced bio-fuel, bio-butanol.^{1–3} The selective conversion of ethanol to butanol is, however, not trivial since the starting material and product have the same chemical functionality; thus, butanol and any higher alcohol are also susceptible to condensation. Both heterogeneous and homogeneous catalysts have been reported to facilitate the Guerbet reaction.^{4–6} Thus far, heterogeneous catalysts have not presented any selectivity for butanol formation.⁶ However, a series of reported homogeneous catalysts have shown some selectivity for 1-butanol (Fig. 1).^{4,7–13}

Currently, the fundamentals of this selectivity are not yet fully understood, and this gap in knowledge motivated us to investigate the reaction mechanism of one of the most selective homogeneous catalysts (**1-Ru**, Fig. 1).¹⁰ The Guerbet mechanism is commonly accepted to proceed through three key steps: dehydrogenation of an alcohol to an aldehyde; aldol condensation of the unsaturated intermediate; and hydrogenation of the aldol product to higher alcohol (Scheme 1A). Notably, previous work showed that bis(pyridylimino)-isoindolate Ru(II) complexes, such as **1-Ru**, can reversibly hydrogenate acetophenone using molecular

hydrogen or isopropyl alcohol as a hydrogen substitute.^{14,15} However, the mechanism of **1-Ru** has not been investigated for the Guerbet reaction, and the precise pathway for the (de) hydrogenation reaction remains unclear. To better understand the mechanism of **1-Ru** for the Guerbet reaction, we independently investigated key reaction steps. To that end, we built a flow reactor setup that allowed us to analyze the catalyst's activity under quasi-steady-state conditions without altering its chemical structure. Ethanol conversion to butanol was monitored for hours on stream where stable activity, up to 10 hours, was achieved. After establishing that the catalysis is not mass transfer limited, a detailed study on the reaction mechanism was performed. First, we established that this catalyst does not present any selectivity for 1-butanol formation under our reaction conditions by comparing our catalytic results to those of a random step-growth model. Second, we determined that **1-Ru** predominantly operates through a transfer hydrogenation pathway and that β -hydride elimination is the rate-limiting step of the reaction (Scheme 1B).

Customarily, homogeneous Guerbet catalysts are studied in closed batch vessels under elevated temperatures and pressures, but these conditions make kinetic studies tedious, especially when considering multi-phase reactants and products. Inspired by the steady-state kinetic analyses of heterogeneous catalysts in flow systems, we developed a flow reactor as an alternative to a classical batch set-up for the investigation of a homogeneous Guerbet catalyst.^{16,17} Flow reactor set-ups offer several advantages, including continuous and automated sampling, facile control over the reaction residence time, and increased chemical safety. Moreover, the

Department of Chemical and Biomolecular Engineering, University of Illinois at Urbana-Champaign, Urbana, IL 61801, USA. E-mail: guironne@illinois.edu

† Electronic supplementary information (ESI) available. See DOI: 10.1039/d1re00551k

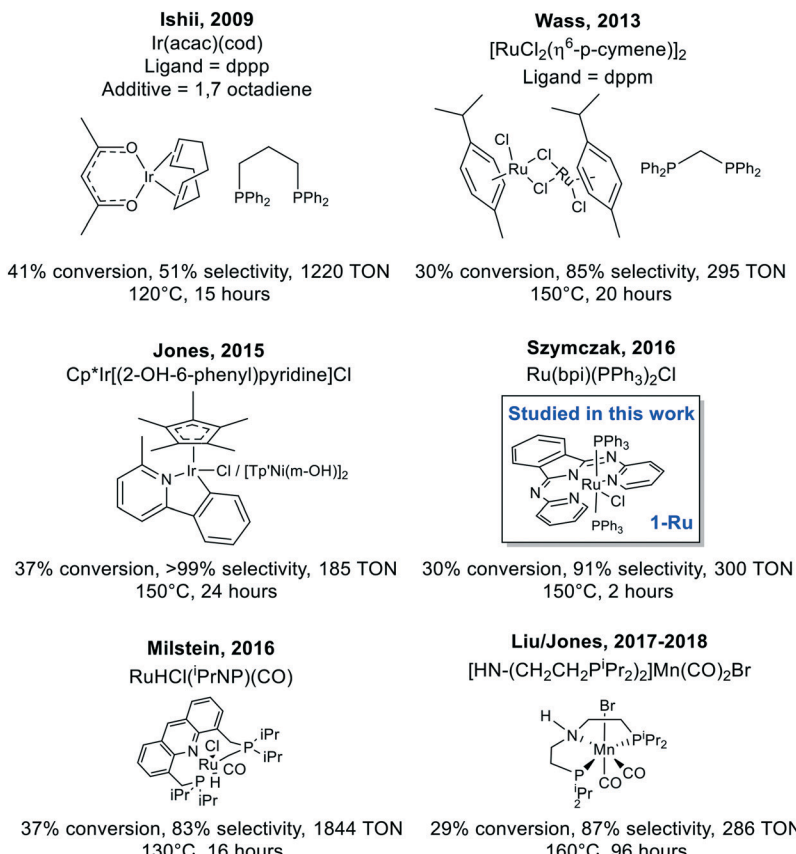
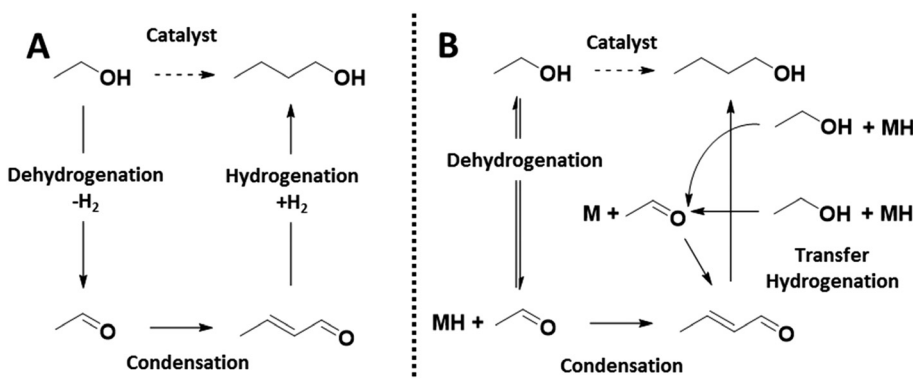


Fig. 1 Recent developments for homogeneous Guerbet catalysts. Ethanol conversion and butanol selectivity are tabulated and summarized.

real-time analysis of all reaction intermediates and the evolution of product distributions provide unique insights into the reaction mechanism that are not easily accessed *via* batch experimentation. To study **1-Ru** under flow conditions, we developed an immobilization strategy that maintains **1-Ru** in a reactor while continuously feeding and extracting reagents and products. The most common approach to catalyst immobilization involves anchoring of the catalyst onto a macroscopic support.^{18,19} While this strategy successfully immobilizes the catalyst, it requires modification

of the ligand structure which can alter the reactivity of the catalyst and can be synthetically intensive.²⁰ Modeling after industrial processes that use homogeneous catalysts in continuous flow reactors (*e.g.* shell higher olefin, Ruhrchemie/Rhône-Poulenc, and Monsanto/Cativa processes), we opted to implement a methodology which relies on thermodynamic equilibrium to separate the volatile reaction components from the non-volatile catalyst.²¹⁻²³ This technique is advantageous as it does not require chemical modification of the catalyst and is applicable to any



Scheme 1 (A) Describes the commonly proposed Guerbet mechanism which proceeds through the reaction of molecular hydrogen. (B) Describes the Guerbet mechanism which proceeds *via* transfer hydrogenation. "M" represents a metal catalyst.

homogeneous catalyst. In our approach, the catalyst is dissolved in a non-volatile solvent and heated in a continuously stirred tank reactor (CSTR, Fig. 2). Volatile substrates are then continuously fed into the system where they react with the catalyst in the condensed phase. The unreacted substrates, reaction intermediates, and products are evaporated and swept by a carrier gas to an in-line gas chromatograph for analysis (see the Reactor Setup and Equipment section in the ESI† for more detail). The outlet stream is open to the atmosphere.

Results

Material compatibility

The immobilization of our catalyst through a vapor-liquid equilibrium (VLE) required the implementation of a non-volatile liquid phase, which led us to investigate polymers as solvents.^{24,25} We first probed the impact of various polymers on the activity of **1-Ru** for ethanol condensation reactions performed in batch (Table 1), and due to the large amount of co-catalyst (sodium ethoxide) needed to activate **1-Ru** we initially focused on hydroxyl containing polymers. The presence of hydroxyl groups proved to be detrimental to the catalysis where a notable decrease in activity (TON, mol_{butanol} mol_{cat}⁻¹) was observed upon the addition of polyvinyl phenol and polyvinyl alcohol. The decrease in activity was rationalized by the increased acidity of the reaction mixture and the protonation of the co-catalyst. These observations led us to select a low molecular weight polyethylene glycol (PEG, MW = 500 g mol⁻¹) to serve as the reaction solvent. PEG was thought to be a good solvent because of its strong affinity for alkali ions which would presumably allow us to solubilize a large amount of co-catalyst.²⁶ The stability of **1-Ru** in PEG was further established in a series of ethanol coupling experiments performed in batch, in which stable catalytic activity was observed for up to 10 hours (Fig. S2†). Moreover,

Table 1 Batch condensation of ethanol to butanol by **1-Ru** in the presence of polymers^a

Entry	Additive	TON (n _{C₄} /n _{cat})
1	Control	145
2	Poly-vinyl phenol	25
3	Poly-vinyl alcohol	100
4	PEG	150

^a All reactions were carried out for 4 hours at 150 °C in 0.4 mL of EtOH with the addition of 50 mg EtONa, 3.5 mg of **1-Ru**, and a known quantity of toluene (internal standard). For reactions loaded with polymer, 100 mg of material was introduced to the reaction mixture. Low ethanol conversions (<5 mol%) were maintained, and butanol was the only detected product from the reaction. TON is defined as the moles of butanol produced per mole of catalyst (n_{C₄}/n_{cat}).

NMR analysis of a PEG-**1-Ru** mixture heated to 120 °C for 30 minutes also showed no change in the ³¹P resonance of the ruthenium complex (Fig. S3†). Thus, the combination of these experiments validated that PEG was compatible with **1-Ru**.

Ethanol coupling in the CSTR

The CSTR was loaded with a polymer-catalyst solution which consisted of PEG, sodium ethoxide, and **1-Ru**. The reaction mixture was heated using a hotplate, whereafter liquid ethanol and nitrogen carrier gas were continuously fed into the heated mixture (Table 2). The pressure was kept constant, and the vapor-phase effluent was directed to an in-line gas chromatograph equipped with an FID detector for analysis. In this study, the ethanol conversion was kept low (below 5 mol%) to ensure a quasi-steady-state condition and to reduce the formation rate of higher alcohols. Acetaldehyde, butanol, 2-ethyl-butanol, and hexanol were identified as the major products exiting the reactor (see Fig. 3 for the product distribution and Fig. S4† for the mass balance). Over the course of a 10 hour reaction, butanol formation underwent multiple phases as it gradually increased for the first 2 hours reaching a maximum TOF (mol_{product} mol_{cat}⁻¹ h⁻¹) of 6 h⁻¹ before decreasing and steady at 4 h⁻¹ after 4 hours. The decrease in butanol formation rate coincides with the increased formation rate of C₆ products, TOF of 1 h⁻¹, and

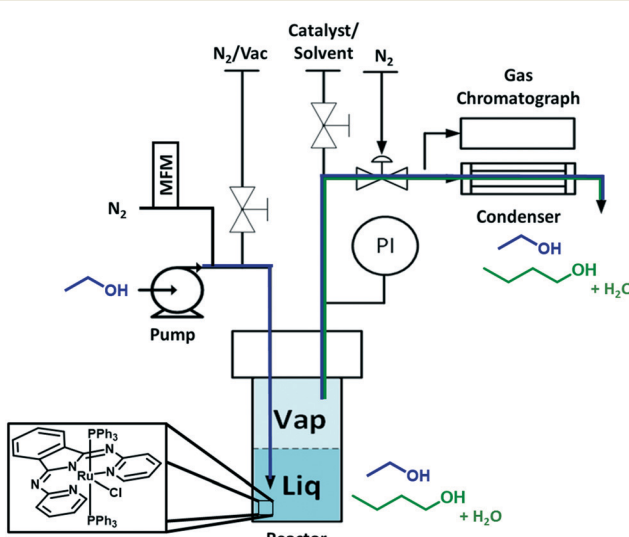


Fig. 2 Schematic for continuous stirred tank reactor design.

Table 2 Standard operating conditions for ethanol condensation reactions in the CSTR^a

Operating Conditions	
PEG	5.33 mL
EtONa	386 mM
1-Ru	0.66 mM
N ₂	8.4 mL min ⁻¹ (g)
EtOH	1.25 μ L min ⁻¹ (l)
Pressure	16 psi
Residence time	35 s
Temperature	120 °C

^a Ethanol conversion for flow coupling is kept below 5 mol% to ensure quasi-steady-state kinetics.

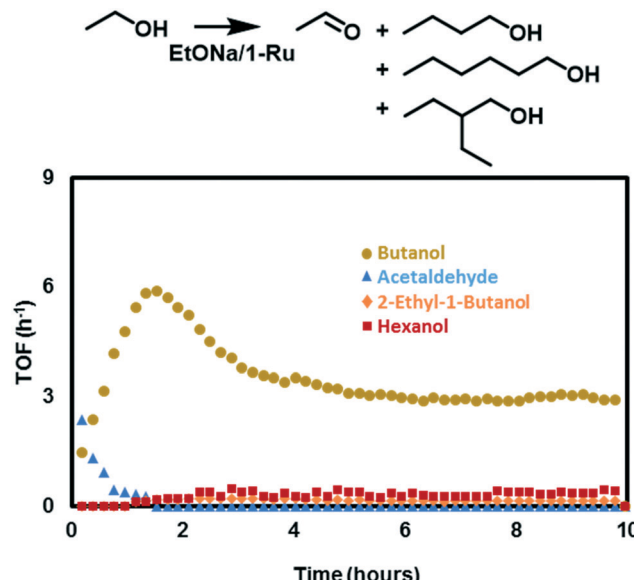


Fig. 3 Product rate profile for ethanol coupling reaction. TOF is defined as the moles of product formed per time per mole of catalyst.

the disappearance of acetaldehyde (see ESI† for sample rate calculations). After several hours on stream, the rate of evaporation and catalysis converged to produce a steady reaction profile. The initial non-monotonic rate of butanol formation was attributed to transient reaction kinetics (see ESI† for qualitative kinetic modeling).

Further analysis of the product distribution also provided valuable insights regarding the selectivity and reaction mechanism of **1-Ru**. First, we compared our experimental C_4/C_6 product ratio ($C_4/C_6 = 4$) to a prediction calculated using a random step-growth condensation model based on Flory's equal-reactivity principle ($C_4/C_6 = 40$, see ESI† for calculations) at equal conversion (2.5 mol%). The higher ratio of C_6 in our experiment led us to conclude that **1-Ru** does not exhibit any selectivity for ethanol coupling under our reaction conditions.²⁷ Our conclusion contrasts with prior reports of the catalyst, and this discrepancy can be, in-part, attributed to the definition of selectivity. Under low conversion conditions, the catalyst is flooded with ethanol as the predominant substrate, which creates an inherent bias for ethanol reaction (butanol formation) over butanol reaction. This provides a false sense of selectivity. We decouple the effect of conversion by comparing the product ratios (C_4/C_6) between a step-growth prediction and our experimental data at identical conversions, which provides a more accurate description of catalytic selectivity.

Second, the absence of unsaturated C_4 intermediates suggests a fast hydrogenation step relative to aldol condensation. This observation was particularly surprising when considering the short residence times (35 s – reaction vol./vol. flow) and the low substrate concentrations. This low substrate concentration is especially true for hydrogen gas due to its higher volatility. Presumably, hydrogen vaporization would result in a non-stoichiometric reaction

Table 3 Condensation of ethanol to butanol by **1-Ru** in the CSTR at different residence times^a

PEG (mL)	Ru (mM)	Residence time (s)	TON ($[n_{C_4} + n_{C_6}]/n_{cat}$)
5.33	0.66	35	60 ± 6^b
6.67	0.66	44	58
6.67	0.50	44	65
6.67	0.33	44	67
8.0	0.66	53	53

^a EtOH and N_2 are fed into the reactor at $1.25 \mu\text{L min}^{-1}$ (l) and 8.4 mL min^{-1} (g) respectively at 120°C and a pressure of 16 psi ($P_{\text{EtOH}} = 0.4 \text{ psi}$). The concentration of sodium ethoxide was held constant at 330 mM for each experiment. ^b Standard deviation was calculated by averaging over three experiments using identical reactor loadings. Butanol, hexanol and 2-ethyl butanol were the predominant products from the reaction. Accordingly, TON is defined as the moles of products formed per mole of catalyst ($[n_{C_4} + n_{C_6}]/n_{cat}$) after 10 hours of reaction time.

that would promote the formation of unsaturated intermediates. However, we did not detect unsaturated C_4 and C_6 molecules in the product stream, which suggested that molecular hydrogen does not play a significant role in the hydrogenation reaction. This conclusion led us to postulate that a transfer hydrogenation reaction is the primary mechanism for the hydrogenation step. Prior to probing our mechanistic hypothesis, it is most important to demonstrate that the reaction performed in the CSTR is not mass transfer limited.

Mass transfer studies

Two potential mass transfer limitations should be considered. First, the transport of ethanol from the bubbles at the inlet to the polymer, and second, the transport of ethanol from the polymer to the head space of the reactor. Mass transfer between the ethanol bubbles and the solvent was studied by varying the PEG loading while maintaining a constant substrate flowrate, co-catalyst concentration, and ethanol partial pressure ($P_{\text{EtOH}} = 0.4 \text{ psi}$). A stainless-steel dip-tube is used to deliver ethanol into the cylindrical reactor. By varying the PEG loadings (5.3–8 mL), we alter the length of the diffusion path from the inlet of the tube to the surface of the polymer (1.2–6.7 mm). Despite varying the diffusion path, the cumulative turnovers over 10 hours of catalysis for

Table 4 Standard operating conditions for C_4 hydrogenation reactions in the CSTR

Operating Conditions	
PEG	5.33 mL
EtONa	386 mM
1-Ru	1.12 mM
He	100 mL min^{-1} (g)
ⁱ PrOH	$20 \mu\text{L min}^{-1}$ (l)
Unsaturated C_4	1 mol% in ⁱ PrOH
Pressure	16 psi
Residence time	0.05 s
Temperature	120°C

Transfer Hydrogenation

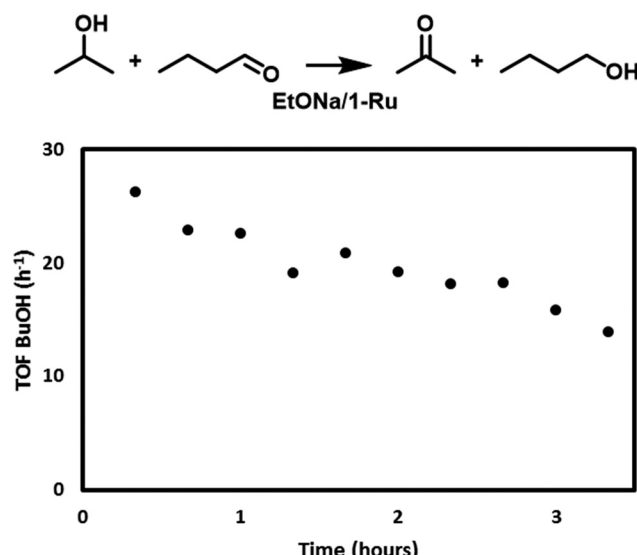


Fig. 4 Butanol formation rate reported over time for the transfer hydrogenation of butyraldehyde.

these experiments remained constant (60 ± 6 TON), suggesting that the rate of mass transfer is rapid in comparison to the Guerbet reaction (Table 3). In addition, we also varied the concentration of **1-Ru** (0.66–0.33 mM) and no change in catalytic rate was observed, providing further confirmation that the concentration of ethanol is constant throughout the liquid phase. Next, mass transfer effects between the liquid phase and the headspace were probed by varying the stir-bar's rate of rotation. An increase in rotation rate creates a vortex with a larger surface area. For a mass transfer limited system, a surface area increase would consequently accelerate the rate of mass transfer and the rate of product formation. However, no enhancement to the alcohol formation rate was observed while periodically increasing the rate of rotation (500–1000 RPM) during a 10 hour experiment, suggesting that transport between phases is rapid and not rate-limiting (Fig. S6†).

Hydrogenation of unsaturated molecules

To probe our hypothesis that the reaction proceeds predominantly through a transfer hydrogenation mechanism we performed a series of hydrogenations on unsaturated C₄ intermediates in the presence of a hydrogen donor, isopropyl alcohol (Table 4). Dilute mixtures of unsaturated C₄ intermediate in isopropyl alcohol were continuously fed as a liquid into the heated CSTR which contained a polymer-catalyst mixture. Helium carrier gas was used to sweep the vapor-phase effluent to the in-line gas chromatograph for analysis of the reaction progress.

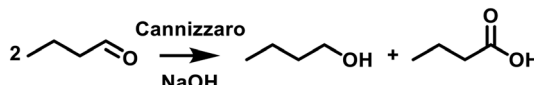
We first studied the transfer hydrogenation of butyraldehyde in the presence of excess isopropyl alcohol. In this experiment, we observed an initial butanol formation rate of 26 h⁻¹ which gradually decayed over 3 hours (Fig. 4 and S14†). Further examination of the product distribution showed a high conversion of butyraldehyde to butanol (59.5 mol%, Table 5). Notably, however, 30.6 mol% of the substrate fed into the reactor was unaccounted for in the gas-phase mass balance. The missing substrate was attributed to the formation of low volatility products *via* aldol condensation and the commonly reported base-catalyzed Cannizzaro disproportionation reaction (Scheme 2).^{28,29} The low volatility products were identified in batch experiments by performing the cross condensation of butyraldehyde and acetaldehyde catalyzed by sodium ethoxide in the absence of **1-Ru** at 120 °C (Table S1†). In particular, the acidic products from the Cannizzaro reaction (acetic and butyric acid) will consume the co-catalyst to form non-reactive sodium salts. Under our flow reactor conditions, the acids (formed continuously *in situ*) react quickly with the high concentration of sodium ethoxide which is consistent with the observed decay in catalyst activity.

Acetone was also detected in the gaseous product stream during the butyraldehyde transfer hydrogenation reaction with an average TOF of 18 h⁻¹ over 3 hours (~1 mol% conversion of isopropyl alcohol). Comparing rates of acetone and butanol formation (Table 5 and Fig. S17†) we noted that the ratio of rates was near unity ($R_{\text{Butanol}}/R_{\text{Acetone}} = 1.1$). This

Table 5 Summary of transfer hydrogenation reactions^a

	Substrate	Butyraldehyde	Crotyl alcohol	Crotonaldehyde
Products (mol%)	Butyraldehyde	9.9	n.d.	2.2
	Crotyl alcohol	n.d.	57.9	1.2
	Crotonaldehyde	n.d.	n.d.	1.5
	Butanol	59.5	37.8	16.2
	Missing C ₄	30.6	4.3	78.9
Rate (h ⁻¹)	R_{Butanol}	20	13	12
	R_{Acetone}	18	25	16
	$R_{\text{Butanol}}/R_{\text{Acetone}}$	1.1	0.5	0.8

^a The table depicts the distribution of intermediates detected at the reactor outlet for transfer hydrogenation reactions while employing different hydrogenation substrates. The formation rate of butanol and acetone are also compared. Note, the conversion of ⁱPrOH does not exceed 2 mol% for all experiments, and the reported data were aggregated by averaging the product formation rates over 3 hours of flow catalysis. Rate is defined as the moles of product formed per time per mole of catalyst. Refer to Fig. S14–S20† for the gaseous product profiles and for the comparison of acetone and butanol formation rates over time.



Scheme 2 Cannizzaro disproportionation reaction of butyraldehyde.

observation provided additional evidence for a transfer hydrogenation pathway, since at least one molecule of acetone was produced for each unsaturated bond that was hydrogenated. The slightly faster rate of butanol formation was attributed to the Cannizzaro reaction.

Next, we studied the transfer hydrogenation of crotyl alcohol (Fig. 5) where we observed a moderate conversion of the substrate to butanol (37.8 mol%) and an average butanol formation rate of 13 h^{-1} over 3 hours (Table 5 and Fig. S15†). Compared to the rate of butyraldehyde hydrogenation, the hydrogenation of crotyl alcohol was slower, suggesting that $\text{C}=\text{C}$ bonds are more difficult to hydrogenate than $\text{C}=\text{O}$ bonds. Furthermore, the gas-phase mass balance for crotyl alcohol hydrogenation was well-accounted, where 95.7 mol% of the initial feed was either converted to butanol or unreacted. Other unsaturated C_4 intermediates apart from unreacted substrate were not detected (<0.001 mol% conversion). We postulate that the missing substrate (4.3 mol%) is indicative of butanol dehydrogenation to butyraldehyde which subsequently condenses to form low volatility C_8 products. Nonetheless, a well-accounted mass balance was consistent with the inability of crotyl alcohol to react *via* aldol-condensation or Cannizzaro reactions. Moreover, a comparison of the butanol and acetone formation rates revealed that more acetone was being formed than butanol ($R_{\text{Butanol}}/R_{\text{Acetone}} = 0.5$, Table 5 and Fig. S18†). Thus, in addition to transfer hydrogenation **1-Ru** was also presumably dehydrogenating isopropyl alcohol to yield hydrogen gas and acetone, which was confirmed by reacting isopropyl alcohol with **1-Ru** and sodium ethoxide in the flow system (Fig. S20†). In this control reaction, isopropyl alcohol conversion remained below 2 mol%, and acetone was formed at an average TOF of 34 h^{-1} over 3 hours. This reactivity was consistent with the ability of bis(pyridylimino)isoindolate Ru(II) catalysts to perform the dehydrogenation of secondary alcohols.^{14,15} Although these experiments provided evidence for the formation of hydrogen gas during the Guerbet reaction, a thermodynamic analysis (see ESI† for CHEMCAD simulation) of hydrogen solubility in PEG under our reaction conditions revealed that the concentration of hydrogen would be at least three orders of magnitude lower than that of the alcohol substrates. These low concentrations strongly suggest that the hydrogenation of unsaturated intermediates through molecular hydrogen is negligible.

Finally, the hydrogenation of crotonaldehyde was investigated where we observed an average butanol formation rate of 12 h^{-1} over 3 hours (Fig. 6 and S16†). This turnover rate for butanol formation corresponds to two cycles of hydrogenation. Thus, the hydrogenation rate of crotonaldehyde appears comparable to crotyl alcohol despite

Transfer Hydrogenation

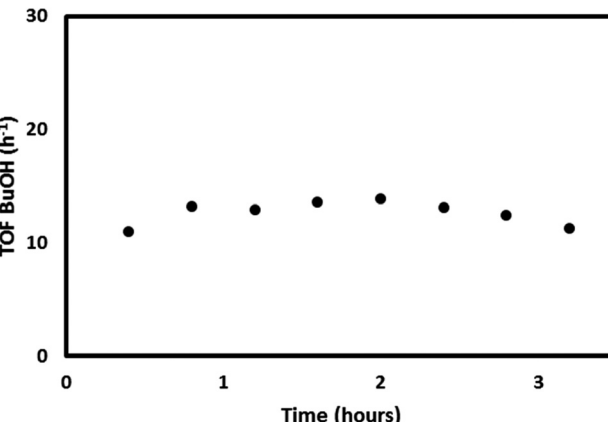
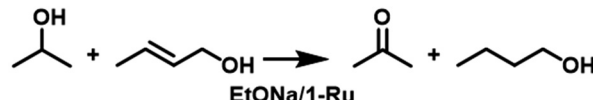


Fig. 5 Butanol formation rate reported over time for the transfer hydrogenation of crotyl alcohol.

the low conversion of crotonaldehyde to butanol (16.2 mol%, Table 5). Only traces of unsaturated intermediates were detected during catalysis (1–2 mol%). Crotonaldehyde was also subject to side-reactions in the presence of sodium ethoxide as evidenced by poor closure of the mass balance where 78.9 mol% of the starting material was unaccounted for in the gas phase. Correspondingly, the acetone and butanol formation rates were less than unity ($R_{\text{Butanol}}/R_{\text{Acetone}} = 0.8$, Table 5 and Fig. S19†).

Transfer Hydrogenation

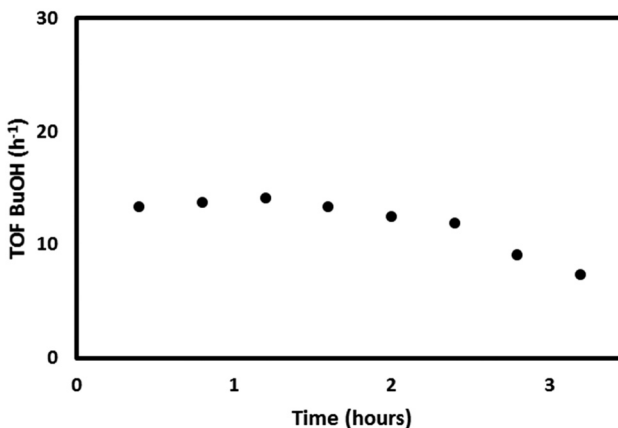
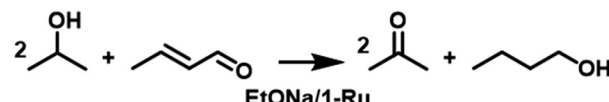


Fig. 6 Butanol formation rate reported over time for the transfer hydrogenation of crotonaldehyde.

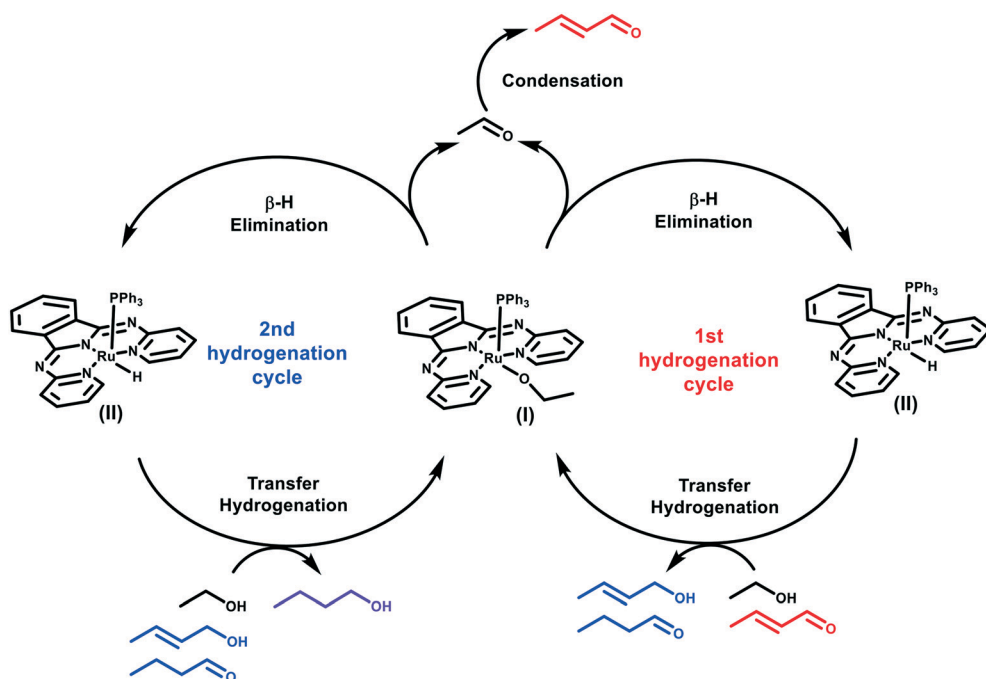


Fig. 7 Simplified Guerbet mechanism mediated by **1-Ru**.

Reaction mechanism

Through our investigations we have provided evidence that the hydrogenation step of the Guerbet reaction mediated by **1-Ru** proceeds predominantly through a transfer hydrogenation mechanism. The absence of detectable unsaturated C_{4+} products during ethanol coupling reactions suggests that transfer hydrogenation is fast. This furthermore implies that condensation must be similarly fast, otherwise no C_6 products would be formed. Overall, these observations point to β -hydride elimination of the ruthenium alkoxy species as the rate-limiting step of the mechanism.⁵ It is worth noting that the hydrogenation rate of unsaturated C_4 in the presence of isopropyl alcohol (Table 5) was faster than the butanol formation rate reported for the Guerbet reaction (Fig. 3). This difference in rate is consistent with the higher reactivity of a secondary alcohol which would more readily undergo β -hydride elimination in comparison to ethanol. A reaction mechanism involving two cycles, one for the monounsaturated and one for the di-unsaturated product is drawn in Fig. 7. Each cycle includes a transfer hydrogenation reaction and a β -hydride elimination step. Finally, we demonstrated that the hydrogenation of unsaturated intermediates through molecular hydrogen is unlikely due to the fast rate of transfer hydrogenation and the low solubility of hydrogen under our reaction conditions. The high concentration of alcohol in a batch reaction would also favor hydrogenation through hydrogen transfer over molecular hydrogen.

Conclusion

Through the development of a flow reactor set-up involving a simple immobilization strategy, we have gained mechanistic

insights into the ethanol self-condensation reaction catalyzed by a homogeneous ruthenium catalyst (**1-Ru**). The methodology allowed us to monitor the reaction progress at steady state for hours. The technique consists of dissolving the catalyst in a non-volatile solvent (a polymer) and leveraging VLE to continuously remove reagents and products of the reaction. The composition of the vapor stream exiting the reaction mixture is analyzed using an inline GC. This technique for catalyst immobilization is particularly powerful as it does not require the modification of the catalyst; and thus, any homogeneous Guerbet catalyst could be used. Stable butanol production was achieved in the reactor for more than 12 hours. By comparing the composition of our product mixture to a prediction from a step-growth polymerization model, we demonstrated that **1-Ru** does not exhibit any selectivity toward butanol formation under our reaction conditions. We also showcased that the hydrogenation step follows a transfer hydrogenation mechanism and that β -hydride elimination of the ruthenium alkoxy is the rate-limiting step of the reaction. Finally, we established that molecular hydrogen, while potentially formed during the reaction, does not participate in the hydrogenation reaction. This combination of reactor engineering and mechanistic insight will help develop next generation catalysts with the goal of identifying catalytic systems that offer high selectivity for ethanol condensation.

Funding sources

The authors thank the NSF CHE 18-00068 for funding.

Author contributions

The manuscript was written through contributions of all authors. All authors have given approval to the final version of the manuscript.

Conflicts of interest

There are no conflicts to declare.

Acknowledgements

Major funding for the 500 MHz Bruker CryoProbe was provided by the Roy J. Carver Charitable Trust (Muscatine, Iowa; Grant #15-4521) to the School of Chemical Sciences NMR Lab.

References

- 1 S. B. Bankar, S. A. Survase, H. Ojamo and T. Granström, Biobutanol: The Outlook of an Academic and Industrialist, *RSC Adv.*, 2013, **3**(47), 24734–24757.
- 2 P. Dürre, Biobutanol : An Attractive Biofuel, *Biotechnology*, 2007, **2**, 1525–1534.
- 3 D. E. Ramey, *U.S. National Agricultural Biotechnology Council (NABC) Reports, Agricultural Biofuels: Technology, Sustainability and Profitability, Part III: Technology: Biomass, Fuels and Co-Products, Butanol: The Other Alternative Fuel*, U. S. National Agricultural Biotechnology Council, Ithaca, NY, 2007, vol. 19, pp. 136–147.
- 4 H. Aitchison, R. L. Wingad and D. F. Wass, Homogeneous Ethanol to Butanol Catalysis - Guerbet Renewed, *ACS Catal.*, 2016, **6**(10), 7125–7132.
- 5 D. Gabriëls, W. Y. Hernández, B. Sels, P. Van Der Voort and A. Verberckmoes, Review of Catalytic Systems and Thermodynamics for the Guerbet Condensation Reaction and Challenges for Biomass Valorization, *Catal. Sci. Technol.*, 2015, **5**(8), 3876–3902.
- 6 J. T. Kozlowski and R. J. Davis, Heterogeneous Catalysts for the Guerbet Coupling of Alcohols, *ACS Catal.*, 2013, **3**(7), 1588–1600.
- 7 T. Matsu-Ura, S. Sakaguchi, Y. Obora and Y. Ishii, Guerbet Reaction of Primary Alcohols Leading to β -Alkylated Dimer Alcohols Catalyzed by Iridium Complexes, *J. Org. Chem.*, 2006, **71**(21), 8306–8308.
- 8 G. R. M. Dowson, M. F. Haddow, J. Lee, R. L. Wingad and D. F. Wass, Catalytic Conversion of Ethanol into an Advanced Biofuel: Unprecedented Selectivity for n-Butanol, *Angew. Chem., Int. Ed.*, 2013, **52**(34), 9005–9008.
- 9 Y. Xie, Y. Ben-David, L. J. W. Shimon and D. Milstein, Highly Efficient Process for Production of Biofuel from Ethanol Catalyzed by Ruthenium Pincer Complexes, *J. Am. Chem. Soc.*, 2016, **138**(29), 9077–9080.
- 10 K. N. T. Tseng, S. Lin, J. W. Kampf and N. K. Szymczak, Upgrading Ethanol to 1-Butanol with a Homogeneous Air-Stable Ruthenium Catalyst, *Chem. Commun.*, 2016, **52**(14), 2901–2904.
- 11 N. V. Kulkarni, W. W. Brennessel and W. D. Jones, Catalytic Upgrading of Ethanol to n-Butanol via Manganese-Mediated Guerbet Reaction, *ACS Catal.*, 2018, **8**, 997–1002.
- 12 S. Fu, Z. Shao, Y. Wang and Q. Liu, Manganese-Catalyzed Upgrading of Ethanol into 1-Butanol, *J. Am. Chem. Soc.*, 2017, **139**(34), 11941–11948.
- 13 S. Chakraborty, P. E. Piszel, C. E. Hayes, R. T. Baker and W. D. Jones, Highly Selective Formation of N-Butanol from Ethanol through the Guerbet Process: A Tandem Catalytic Approach, *J. Am. Chem. Soc.*, 2015, **137**(45), 14264–14267.
- 14 K. N. T. Tseng, J. W. Kampf and N. K. Szymczak, Base-Free, Acceptorless, and Chemoselective Alcohol Dehydrogenation Catalyzed by an Amide-Derived NNN-Ruthenium(II) Hydride Complex, *Organometallics*, 2013, **32**(7), 2046–2049.
- 15 K. N. T. Tseng, J. W. Kampf and N. K. Szymczak, Mechanism of N,N,N-Amide Ruthenium(II) Hydride Mediated Acceptorless Alcohol Dehydrogenation: Inner-Sphere β -H Elimination versus Outer-Sphere Bifunctional Metal-Ligand Cooperativity, *ACS Catal.*, 2015, **5**(9), 5468–5485.
- 16 T. Moteki and D. W. Flaherty, Mechanistic Insight to C-C Bond Formation and Predictive Models for Cascade Reactions among Alcohols on Ca- and Sr-Hydroxyapatites, *ACS Catal.*, 2016, **6**(7), 4170–4183.
- 17 C. R. Ho, S. Shylesh and A. T. Bell, Mechanism and Kinetics of Ethanol Coupling to Butanol over Hydroxyapatite, *ACS Catal.*, 2016, **6**(2), 939–948.
- 18 C. Li and Y. Liu, *Bridging Heterogeneous and Homogeneous Catalysis: Concepts, Strategies, and Applications*, Wiley-VCH, 2014.
- 19 J. W. Niemantsverdriet and I. Chorkendorff, *Concepts of Modern Catalysis and Kinetics*, Wiley-VCH, 2003.
- 20 S. Hübner, J. G. de Vries and V. Farina, Why Does Industry Not Use Immobilized Transition Metal Complexes as Catalysts?, *Adv. Synth. Catal.*, 2016, **358**(1), 3–25.
- 21 W. Keim, Oligomerization of Ethylene to 1-Olefins: Discovery and Development of the Shell Higher Olefin Process (SHOP), *Angew. Chem., Int. Ed.*, 2013, **52**, 12492–12496.
- 22 C. W. Kohlpaintner, R. W. Fischer and B. Cornils, Aqueous Biphasic Catalysis: Ruhrchemie/Rhône-Poulenc Oxo Process, *Appl. Catal., A*, 2001, **221**(1–2), 219–225.
- 23 G. J. Sunley and D. J. Watson, High Productivity Methanol Carbonylation Catalysis Using Iridium. The CativaTMprocess for the Manufacture of Acetic Acid, *Catal. Today*, 2000, **58**(4), 293–307.
- 24 M. L. Harrell, T. Malinski, C. Torres-López, K. Gonzalez, J. Suriboot and D. E. Bergbreiter, Alternatives for Conventional Alkane Solvents, *J. Am. Chem. Soc.*, 2016, **138**(44), 14650–14657.
- 25 C. J. Clarke, W. C. Tu, O. Levers, A. Bröhl and J. P. Hallett, Green and Sustainable Solvents in Chemical Processes, *Chem. Rev.*, 2018, **118**(2), 747–800.
- 26 H. M. Trimble, Solubilities of Salts in Ethylene Glycol and in Its Mixtures with Water, *Ind. Eng. Chem.*, 1931, **23**(2), 165–167.
- 27 P. J. Flory, Fundamental Principles of Condensation Polymerization, *Chem. Rev.*, 1946, **39**, 137.
- 28 S. Cannizzaro, Über Den Der Benzoësäure Entsprechenden Alkohol, *Justus Liebigs Ann. Chem.*, 1853, **88**(1), 129–130.
- 29 V. T. Tishchenko, On the Effect of Aluminium Alkoxides on Aldehydes. Ester Condensation, as a New Kind of Aldehyde Condensation, *Zh. Russ. Fiz.-Khim. O-va.*, 1906, **38**, 355.